Electrocatalysis (2017) 8:67–73
DOI 10.1007/s12678-016-0343-9

ORIGINAL RESEARCH

Beneficial Promotion of Underpotentially Deposited Lead Adatoms on Gold Nanorods Toward Glucose Electrooxidation

Seydou Hebié[1] · **Teko W. Napporn**[1] · **K. Boniface Kokoh**[1]

Published online: 16 November 2016

Abstract Unquestionably, obtaining nanomaterials with high catalytic activity requires the control of their size, shape, and composition since such parameters greatly influence the properties of the electrode surface. In this study, three gold nanorods (GNRs) with different aspect ratios and surface crystallographic orientations were synthesized by wet chemical method. Underpotential deposition (UPD) is an electrochemical technique used with lead adatoms for revealing the low-Miller-index Au(hkl) facets of the as-prepared nanorods. As catalyst effectiveness strongly depends on the nanoparticle surface and the nature of the electrolyte, lead adatom-modified Au electrode materials were made to catalyze the glucose oxidation in alkaline medium in which it is more reactive. It was found that the glucose-to-gluconolactone oxidation peak shifted of 50 mV toward lower potentials, indicating a surface energy gain of the anode material due to the UPD_{Pb} modification.

Keywords Au nanorods · Lead UPD · Electrocatalysis · Glucose oxidation

Introduction

The utilization of active nanomaterials in catalytic amount toward glucose electrooxidation opens an outstanding application route in sensors and hybrid fuel cells [1–4]. In this last decade, significant efforts were made in synthesizing and designing gold nanoparticles (GNPs) that were very selective in the oxidative transformation of aldehydes and hemiacetals such as glucose. This unexpected ability of GNPs was thereby correlated to their size, shape, structure, and composition [2, 4–14]. Such parameters confer to an electrode a specific reactivity allowing surface electron facility to promote a catalytic reaction process [15, 16]. To mitigate the poisoning effect resulted in the organic intermediates strongly adsorbed at active electrode sites, and to improve the glucose conversion efficiency, another metal was often added as co-catalyst to the gold-based material [5–14, 17, 18]. Al, Ag, Cu, Ni, Co, and Pb were successfully combined with Au to obtain a pronounced effect to promote oxygen activation in gold-catalyzed oxidation reactions [13, 18]. Investigations on bulk gold electrode have shown that electrocatalytic glucose oxidation has reaction kinetics, which is from sluggish to fast in acidic, neutral, and alkaline media, respectively [11, 19, 20]. On the standpoint of reaction mechanism and pathway, it is well known that the electrooxidation of glucose proceeds via the dehydrogenation of the anomeric carbon and is strongly dependent on the number of AuOH sites at the electrode surface [2, 3, 12, 17]. To overcome this lack of OH^- species at low electrode potentials, bimetallic Au-Hg was suggested as catalyst for the glucose oxidation because of an increase in the amount of the adsorbed OH^- on the Hg adatom-modified Au electrode [14]. Additionally, it was found that the adsorption of OH species facilitates stronger interaction of glucose with the Hg adatom-modified Au electrode surface by reducing the activation energy of this reaction [14]. More recently, the electrocatalysis of oxygen reduction reaction (ORR) on Pb adatom-modified gold and the oxidation of CO by Pb adatom-modified Pt electrode have been reported [18, 21]. It was found that the gold surface, covered by UPD_{Pb}, was more suitable in terms of oxygen adsorption than a bare gold surface, enhancing thereby the ORR kinetics [18]. UPD_{Pb} has

✉ K. Boniface Kokoh
boniface.kokoh@univ-poitiers.fr

[1] Université de Poitiers, IC2MP UMR-CNRS 7285, 4, rue Michel Brunet B-27, TSA 51106, 86073 Poitiers Cedex 09, France

also a strong screening effect on the adsorption of both H and CO in the Pb-on-Pt network [21]. A few reports concern methods of designing two-dimensional Au-Pb materials with controlled thickness, surface composition, and structure. Amongst them, one can mention the surface limited redox replacement (SLRR) and electrodeposition process from the PbO_2 formation at high-potential range in the presence of lead salt [5–11, 13, 14, 18, 21, 22]. The selective decoration of gold sites by Pb adatoms is an efficient, elegant, and well-controlled way not only to access to a surface formation but also to design new catalysts. However, attention has been paid to Pb-modified Au nanomaterials through direct lead electrodeposition in the underpotential deposition (UPD) potential region for controlling the catalytic layer. This work aims at exploring the ability of the underpotential deposition techniques to successfully and selectively grow Pb particles at the Au surface. Furthermore, we evaluated the synergistic effect of Pb on these materials through the electrooxidation of glucose as model molecule. It demonstrated the beneficial process of lead UPD for characterizing a surface nanostructure and the surfactant removal after PbO_2 deposition/stripping. The excellent activity of Pb-modified gold nanorods (GNRs) was evidenced by cyclic voltammetry which permitted to emphasize the role of Pb in the adsorption of glucose molecule as well as its dehydrogenation at the electrode surface.

Experimental Section

Lead(II) nitrate (99.5%, Merck), NaOH (97%), and D-(+)-glucose (99.5%) were obtained from Sigma-Aldrich®. All reactants were used without any purification.

The cyclic voltammetry studies were carried out in a conventional three-electrode electrochemical glass cell. A slab of glassy carbon (GC) and reference electrode was a reversible hydrogen electrode (RHE) that served as counter and reference electrodes, respectively. The working electrode was a glassy carbon disk of 3 mm diameter mounted in Teflon. Before any electrochemical measurement, the electrolyte was purged with nitrogen to expel dissolved oxygen. The nitrogen flow is maintained during the experiment for avoiding any oxygen introduction in the electrolyte. Prior to each experiment, the GC electrode was polished with alumina 0.5 μm and 0.1 μm, respectively, followed by several ultrasonic cleanings in ultrapure water. Then, a 5 μL volume of the colloidal solution of unsupported GNRs was deposited onto the GC disk, dried under nitrogen atmosphere; thereafter, the working electrode was introduced into the electrolyte under potential control of 0.2 V vs. RHE. All the voltammetric experiments were performed with a potentiostat (EG&G Princeton Applied Research Model 362).

It is well known that the electron transfer kinetics can be strongly affected by the capping agent adsorbed at the gold nanoparticle surface [22]. Thus, after synthesis, the GNR solutions were first cleaned by centrifugation for removing a large amount of excess hexadecyltrimethylammonium bromide (CTAB) surfactant. Then, the few remaining surfactants physically bonded on the surface of the GNRs can be removed electrochemically by potential cycling. This treatment requires much attention in order to avoid any loss of the preferential crystallographic orientation and surface properties of the nanoparticles. Finally, a less aggressive process introduced by Hernández et al. [22] based on PbO_2 deposition/stripping at high potential for the removal of organic capping agents from gold nanoparticle surface in an alkaline solution of lead nitrate was employed in the final cleaning protocol.

Pb-modified GNR electrodes were formed by linear potential scanning from 0.85 to 0.25 V. Following this deposition step, the modified electrodes were rinsed three times with ultrapure water prior to glucose electrooxidation experiments.

Results and Discussion

Physical Characterization of the As-prepared GNR Materials

Three types of GNRs were synthesized by three different growth processes, namely seed-mediated growth process for GNRs-A sample, in situ seed production for GNRs-B sample, and one-step method, using β-diketone as reducing agent, for GNRs-C one. The details of these synthesis methods are well described in the literature [4]. Morphologically, the aspect ratios of 3.3, 2.5, and 4.2 were obtained for the synthesized GNRs-A, GNRs-B, and GNRs-C, respectively. Figure 1 shows the TEM and HRTEM images of the three synthesized GNRs. As can be observed, the particles are quite uniform in shape and size as expected. The high-resolution TEM images clearly exhibit that the lateral faces of the rods consist of stairs, while the end faces are mainly composed of (100) and (111) index facets (with d_{111} in the core of 0.235 nm).

For GNR catalysts, as the crystallographic facets exposed to the electroreactive species constitute the key factors in determining the catalytic activity of nanoparticles, the following investigation of the electrode surface by sensitive cyclic voltammetry is helpful and suitable for the characterization of unmodified GNRs (surfactant-free) as well as Pb-modified GNR materials.

Electrochemical Surface Cleaning and Characterization of GNRs

Since the GNR samples were synthesized in the presence of CTAB, a film of the surfactant covers their surface. This even determines the unidimensional growth mechanism of the nanorods. Additionally, the adsorption of such molecules is

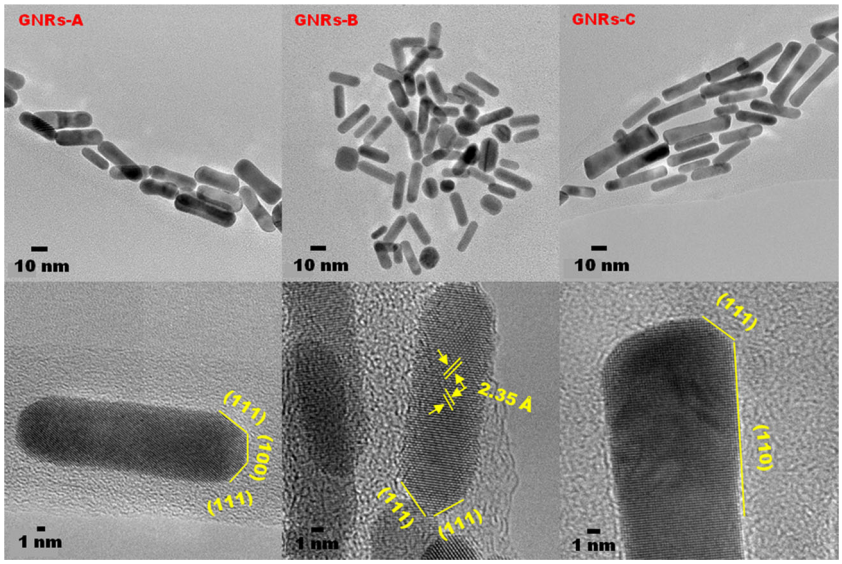

Fig. 1 Transmission electron micrographs (TEM) and HRTEM of **a** GNRs-A, **b** GNRs-B, and **c** GNRs-C

surface sensitive [22]. As the electrocatalytic activity of the gold nanoparticles can be significantly affected by the adsorbed organic species, their cleaning before any electrochemical study is crucial. From a practical point of view, such cleaning process does not alter the surface structure of the catalytic materials. Because of its high sensitivity to the surface, the UPD_{Pb} experiments were conducted to reveal and quantify the crystallographic structure of GNRs and finally to associate it with the electrocatalytic properties of the gold nanorods [22]. The UPD technique involves the deposition of a Pb monolayer on a foreign substrate at potentials more positive than the thermodynamic electrode potential of Pb^{2+}/Pb couple. This could possibly facilitate the formation of bimetallic composition surface since it depends on the specific interaction between the surface atoms of the supporting metal and the deposited lead atoms.

Figure 2 shows UPD_{Pb} on GNRs-A in 0.1 mol L^{-1} NaOH + 1 mmol L^{-1} $Pb(NO_3)_2$ at 20 mV s^{-1} at 20 °C. In the low-potential region, $E < 0.7$ V vs. RHE, during the negative scan, two deposition peaks of lead on (110) and (111) facets were observed around 0.52 and 0.39 V, respectively. In contrast, during the positive potential sweep, three stripping peaks corresponding to the desorption of lead layer on (111), (100), and (110) facets were observed at around 0.41, 0.47, and 0.57 V, respectively. The charge related to UPD_{Pb} depends on the nature of the crystallographic facet. For example, an evaluation of the percentage of lead on GNRs-A surface gives respectively 19.53% of Au(111), 7.23% of Au(100), and 73.24% of Au(110) if one considers a total charge of 440 μC cm^{-2}, which corresponds to the formation of a Pb monolayer on the polycrystalline gold electrode as previously reported [22]. As a result, the ratio between the total charge density calculated from both deposition and desorption peaks gives the coverage on each material. It is clearly observed that the deposition of the lead on Au surface depends on the type of the GNRs (crystallographic structure and aspect ratio). For example, the charges associated with the deposition of lead on GNR materials are 215.6, 140.8, and 686.4 μC cm^{-2} for GNRs-A, GNRs-B, and GNRs-C, respectively. From these values, the surface coverage was calculated by dividing the charge corresponding to the deposition of Pb by the theoretical charge of 440 μC cm^{-2} which corresponds to the charge related to the deposition of a monolayer of Pb on polycrystalline gold electrode. Thus, the coverage assessed for GNRs-A, GNRs-B, and GNRs-C is 0.49, 0.32, and 1.56, respectively, indicating that the lead adlayer tends to be a hexagonal incommensurate for GNRs-A and GNRs-B electrodes and an arrangement in hexagonal compact for GNRs-C. Thus, the deposition of Pb atom leads probably to create a coreshell network with some structure defects where the Au nanorods constitute the core and Pb atoms, the shell.

It was demonstrated that the deposition of a PbO_2 film in alkaline solution contributes to the removal of impurities from the gold surface without any alteration of the crystallographic surface domains of the particles [22]. In the high-potential region ($E > 1.0$ V), in the presence of Pb^{2+}, the voltammogram corresponds to the "cleaning" treatment on a GNRs-A at 20 mV s^{-1} (Fig. 2). During the anodic scan at a high potential value, two peaks are observed at ca. 1.10 and 1.45 V corresponding to the formation of the Pb_3O_4 and PbO_2 layers [18]. Thus, the PbO_2 deposition may protect the gold surface of further oxidation at higher potentials. During the negative scan, the lead oxides are partially stripped off at two distinct peaks C'1 and C'2, respectively. Such peaks were previously observed for small-size spherical gold nanoparticles. Regarding peak C'2, it corresponds in part to the deposition of Pb at (111) facet and the residual trace of unreduced lead oxide. It can be observed that other faradaic processes take

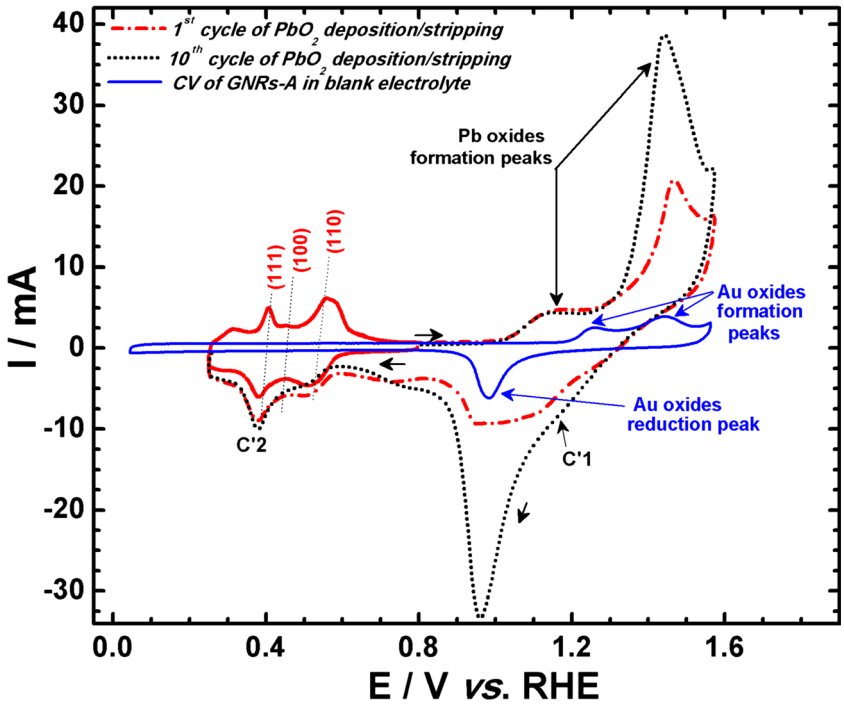

Fig. 2 Cyclic voltammograms of GNRs-A electrode in 0.1 mol L^{-1} NaOH (*solid line*) and first and tenth cycles of the cleaning process in 0.1 mol L^{-1} NaOH + 1 mmol L^{-1} $Pb(NO_3)_2$ at 20 mV s^{-1}, *dash-dotted line* and *dot line*, respectively. Underpotential deposition of lead over the same electrode at low-potential region (*solid line* of potential region between 0.25 and 0.85 V)

place at the potential region of C'2 since the signal is much larger than the UPD one. The ratio of the reductive charge in the reverse scan to the anodic charge in the forward scan is around 0.63. Peak C'2 is related to both lead UPD on gold nanoparticles and the partial dissolution of lead oxide species, PbO_2, i.e., the formation of soluble lead species in the forward scan that diffuses toward the bulk solution, as previously observed [18]. The evolution of such peaks in electrolyte containing the glucose molecule will be further discussed in the following section. The slight increase in the lead deposition and dissolution peak current after the lead oxide film deposition and dissolution was observed showing that a small amount of surface surfactant has been removed from the GNR surface in agreement with the literature [22].

Lead Adatom-Modified GNR Electrodes Toward the Oxidation of Glucose

After the electrodeposition step, the electrode was rinsed three times with ultrapure water and rapidly introduced in another cell containing a fresh 0.1 mol L^{-1} NaOH electrolyte and 10 mM glucose. In order to gain further insight into the synergistic effect of the Pb adatom-modified electrodes on the glucose oxidation, prolonged cyclic voltammetry (CV) tests of 20 cycles were conducted on such anode GNRs. During the potential cycling, the electrocatalytic performance gradually increases with the number of cycles and the onset potential also slightly shifts toward lower values. The activity is much attenuated at the first cycle suggesting a blocking effect of the Pb atoms. This result indicates that a high coverage of the Au surface by the Pb adatoms may inhibit the accessibility to the actives sites and prevent the adsorption of glucose at the AuOH sites. During the potential cycling, the physisorbed UPD_{Pb} are gradually removed while the strong Au-Pb bonds are rearranged at the Au surface allowing the glucose adsorption. The dissolution of a part of the Pb adatoms in the initially deposited compact layer may create some structural defects that promote the accessibility and adsorption of the glucose molecule on GNR surface. Actually, during the potential cycling, the surface composition and structure change with the repeated oxidation/reduction of the surface of the electrode, as evidenced in Fig. 2. For example, during the forward potential scan, the surface tends to Au and Pb oxides (AuO or Au_2O_3 and PbO or PbO_2, respectively). These surface redox processes strongly affect the catalytic properties of the anode material because the adsorption of OH species facilitates stronger interaction of glucose with the Pb adatom-modified Au electrode surface by reducing the activation energy of this reaction. Y. Wang et al. [18] have shown that a "shell" of lead oxides can remain on some gold nanoparticles after the PbO_2 deposition/stripping step. It is now obvious that the Pb traces remaining adsorbed at the host material sites as gold or platinum have strong catalytic effect on the glucose oxidation reaction by the "activation" of the electrode surface. Therefore, the selectivity of the glucose oxidation reaction can be improved [20]. The activity gradually increases and reaches the maximum after 10–13 voltammetry cycles over 0.05–1.6 V (Fig. 3a). The glucose-to-gluconolactone dehydrogenation on GNRs becomes easier thermodynamically when the peak potential shifts of 50 mV toward the lower potentials in

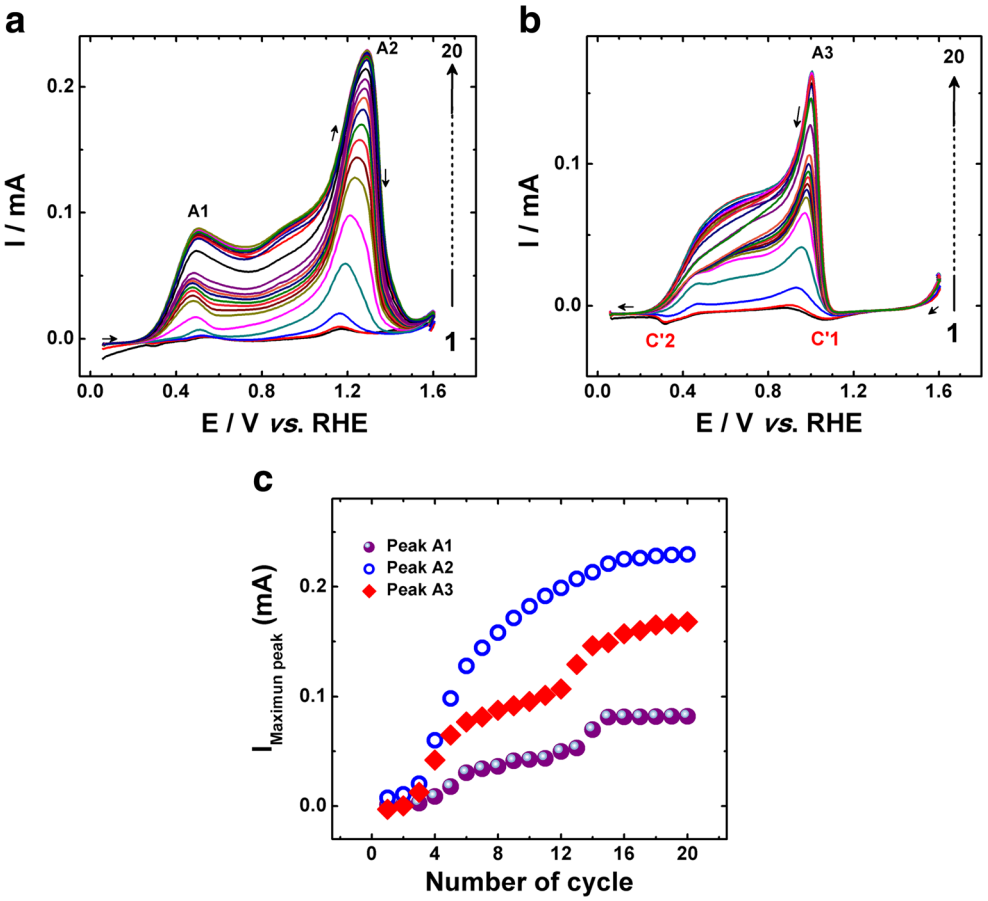

Fig. 3 Successive voltammograms of GNRs-A recorded during the **a** forward and **b** backward potential scans in the presence of 10 mmol L^{-1} glucose. **c** Peak maximum current intensity evolution as function of the number of voltammetric cycles

comparison to the values observed on unmodified Au electrodes. This result indicates that the reaction kinetics is more favorable at the Au-Pb surface particularly with low Pb adatom content at the electrode surface [21].

Considering that the enhancement is due to the presence of Pb adatoms, several factors can be taken into account to explain the catalytic activity observed on the Pb-modified GNR electrodes. Figure 3b shows the successive cyclic voltammograms of Pb-modified GNRs-A for glucose oxidation during the negative potential-going scan. Two small peaks were noticed at 1.06 V (peak C'1) and 0.32 V (peak C'2), corresponding to the PbO_2 reduction and Pb stripping at (111) facet, respectively [23]. The current intensities of these peaks progressively increase up to the 20th cycling. At these quasi-steady state conditions, the oxidation peak at 1.06 V reaches its maximum value (0.25 mA) and peak C'2 becomes a shoulder of glucose dehydrogenation. As shown in Fig. 3c, this good ability of the electrode toward the glucose conversion as function of cycling is probably due to the combined effect of the complete removal of the surfactant molecules by CV and the presence of Pb on the Au surface through the UPD_{Pb}. One can explain this behavior by the bifunctional effects resulting from the coreshell-type network (Pb-on-Au).

The kinetic, thermodynamic, and structural aspects of the UPD_{Pb} and their stability on the gold surface have been intensively studied [24–27]. Hamelin et al. [25] provided evidences of the strong dependence of the adsorption of Pb atoms on the crystallographic orientation of the gold substrate. In the UPD process, bulk metal deposition is preceded by the gradual build-up of a monolayer or of a submonolayer at potentials more positive than the reversible Nernst potential of the bulk deposition. It is shown that in the sorption process, the Pb^{2+} transfer occurs dominantly at the lattice sites or active centers, evolving local gradients that are levelled out by surface diffusion [27]. Thus, the Pb adatoms switch to island growth at the Au surface in order to minimize the elastic strain energy and surface energy of the ensemble. The growth species are more weakly bounded to each other than the substrate. For instance, the adsorbate-substrate, i.e., Pb-Au, interactions are stronger than the adsorbate-adsorbate ones, leading to the formation of adatom islands. However, the desorption of some weak-adsorbed or weak-physisorbed Pb atoms from the Au nanoparticle surface can be due to the weak interactions between Pb atoms.

By overlaying in Fig. 4a the voltammograms of the two investigated electrode materials, it can be observed that the

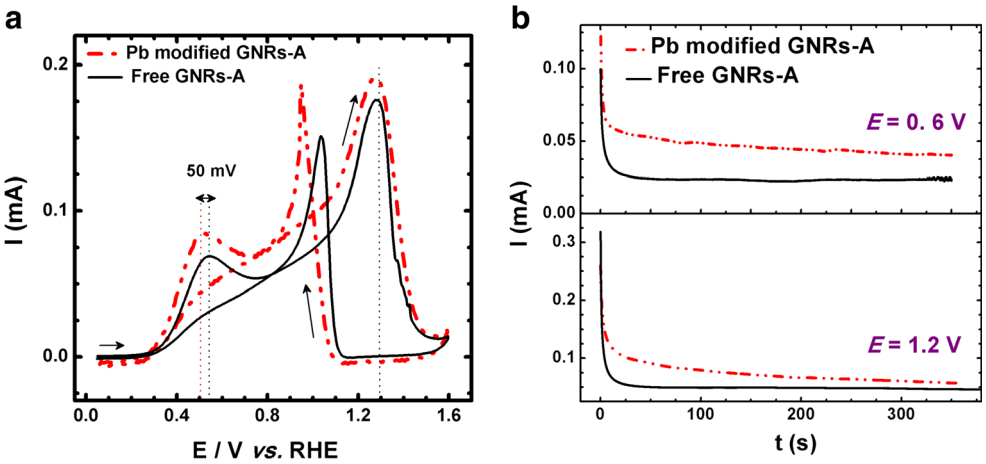

Fig. 4 **a** Voltammograms of GNRs-A (*solid line*) and Pb adatom-modified GNRs-A electrode (*dashed line*) in 0.1 mol L^{-1} NaOH + 10 mmol L^{-1} glucose at 50 mV s^{-1}. **b** Chronoamperometric curves at electrode potentials of 0.6 V (*top*) and 1.2 V vs. RHE (*bottom*) for 350 s

Pb-modified GNRs-A electrode is more active than the free GNRs-A one toward the glucose oxidation in terms of current intensity. As the onset potential does not shift markedly toward lower values, one can more explain the enhancement of the glucose oxidation currents by a preferential adsorption of lead adatoms on the easily poisoning sites of the gold electrode. As these features concern all the glucose oxidation peaks mentioned above, chronoamperometric measurements were performed at two potential regions, the first at 0.6 V and the second one in the oxide potential domain at 1.2 V (Fig. 4b). Concerning the shape in current of both polarization curves, one can notice an initial abrupt decay that may result from the catalyst poisoning by organic species chemisorbed onto the Au sites. At the plateau region, the current densities of the Pb-modified GNRs-A are 1.3 to two times higher than those found at the surface of GNRs-A. All the investigated catalysts display similar current decay shape. The enhancement in the electrocatalytic activity during the potential cycling has three main origins. The first one is due to an increase in the number of the active sites by the cleaning effect of PbO_2 treatment as result of the removal of the surfactant at Au surface [5]. The second one results from the gradual activation of Pb surface, namely the electronic effect of Pb adatoms in electroactivity of Pb-on-Au electrodes, as recently reported [28]. In fact, W. Zhang et al. [28] has shown that the high-charge transfer reaction in the bifunctional electrode materials composed of Pb dispersed in capacitive activated carbon (AC) is due to the gradual rearrangement of the electrodeposited lead on the surface of AC, forming bulk Pb, resulting in enhanced electrochemical surface area [28]. Otherwise, in Pb-on-Au catalysts, since gold has the highest electronegativity 2.54 against 2.33 for lead, electron transfer from Pb to Au may occur, which will slightly affect the catalytic performance of gold. The physical origin of the synergy between two metals is also ascribed to (geometric) ensemble effects. Therefore, both electronic and ensemble effects may conjointly contribute to improve the stability of such electrode materials.

The electrocatalytic effect obtained by underpotential deposition of Pb adatoms is evidenced in Fig. 5 which gives the ratio of current *I* (Pb-modified GNRs)/*I* (GNRs), with and without Pb adatoms, during the forward potential scan. The results show a strong dependence of the electrocatalytic activity of glucose oxidation with the amount of Pb adatoms on GNR surface. The activity is lower for GNRs-B and GNRs-C containing 0.32 and 1.56 monolayer (ML) of Pb, respectively. No apparent electrooxidation of glucose enhancement takes place, the activation and kinetics on such Pb-modified GNRs being effectively the same as on unmodified ones (See Electronic Supplementary Material). The strong electrooxidation activity is obtained with Pb-modified GNRs-A electrode which contain 0.49 ML of Pb. In fact, changes in Pb content result in a slightly negative shift in the potential of the peak of glucose dehydrogenation that scales with the increase of Pb content. Once again, these results suggest electronic and

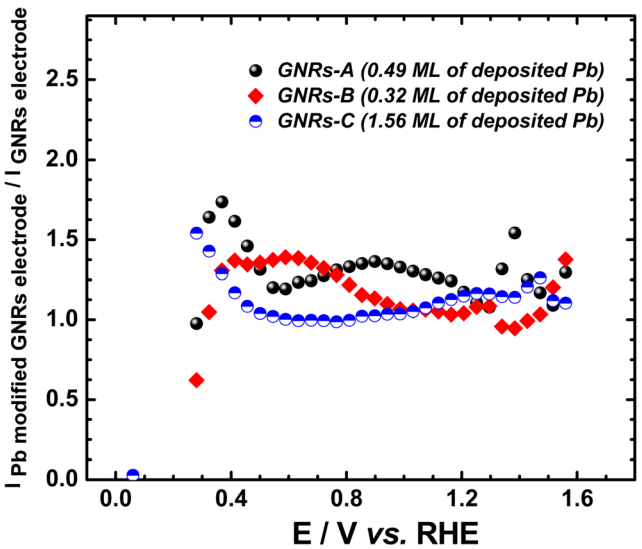

Fig. 5 Electrocatalytic effect of Pb adatoms on the glucose oxidation during the forward potential scans for different GNR electrodes

bifunctional effects of incorporated Pb on the electrochemical behavior of GNRs. Similarly to the literature, the dependence of the underpotential deposition of lead on gold nanoparticles is found to be related to the ORR catalysis and on the adsorption of both H and CO [18, 21].

Conclusion

In summary, the electrooxidation of glucose was studied in alkaline medium at the GNR and Pb-modified GNR catalysts. It was evidenced by electrochemical measurements, the ability of making bimetallic-like coreshell network (Pb-on-Au) materials via the utilization of an in situ UPD_{Pb} process. Pronounced catalytic effects emphasized by underpotential deposition of lead adatoms were observed; it was found that the complete Pb layer could have an inhibitory effect, i.e., the blocking of active sites on the electrocatalytic activity toward the glucose electrochemical transformation. Conversely, the Pb-on-Au with low coverage promotes the reaction rate leading to a 1.3 to two times higher activity than free GNR electrode materials. Indeed, the revelation of the GNR surface showed that the lead adatoms removed well the surfactant molecules resulted from the synthesis approach; by cleaning the active GNR sites and based on the ensemble and bifunctional effects resulted in the coreshell-type network (Pb-on-Au), the glucose oxidation undergoes less poisoning at any potential region and displays higher current densities.

Acknowledgements The authors acknowledge the CNRS and the Region Poitou-Charentes for their financial support.

References

1. D. Feng, F. Wang, Z. Chen, Sens. Actuator B-Chem **138**, 539 (2009)
2. S. Hebie, T. W. Napporn, C. Morais, K. B. Kokoh, ChemPhysChem **17**, 1454 (2016)
3. S. Hebié, Y. Holade, K. Maximova, M. Sentis, P. Delaporte, K. B. Kokoh, T. W. Napporn, A. V. Kabashin, ACS Catal. **5**, 6489 (2015)
4. S. Hebié, K. B. Kokoh, K. Servat, T. W. Napporn, Gold Bull. **46**, 311 (2013)
5. O. Hazzazi, C. Harris, P. Wells, G. Attard, Top. Catal. **54**, 1392 (2011)
6. M. Tominaga, T. Shimazoe, M. Nagashima, H. Kusuda, A. Kubo, Y. Kuwahara, I. Taniguchi, J. Electroanal. Chem. **590**, 37 (2006)
7. M. Tominaga, T. Shimazoe, M. Nagashima, I. Taniguchi, Electrochem. Commun. **7**, 189 (2005)
8. S. Cho, H. Shin, C. Kang, Electrochim. Acta **51**, 3781–3786 (2006)
9. C. C. Jin, I. Taniguchi, Chem. Eng. Technol. **30**, 1298 (2007)
10. P. Tonda-Mikiela, T. W. Napporn, C. Morais, K. Servat, A. Chen, K. B. Kokoh, J. Electrochem. Soc. **159**, H828 (2012)
11. K. B. Kokoh, J. M. Léger, B. Beden, C. Lamy, Electrochim. Acta **37**, 1333 (1992)
12. M. W. Hsiao, R. R. Adžić, E. B. Yeager, J. Electrochem. Soc. **143**, 759 (1996)
13. A. Wang, X. Y. Liu, C.-Y. Mou, T. Zhang, J. Catal. **308**, 258 (2013)
14. F. Matsumoto, M. Harada, N. Koura, S. Uesugi, Electrochem. Commun. **5**, 42 (2003)
15. B. Wu, N. Zheng, Nano Today **8**, 168 (2013)
16. Z. Guo, X. Fan, L. Liu, Z. Bian, C. Gu, Y. Zhang, N. Gu, D. Yang, J. Zhang, J Colloid Interf Sci **348**, 29 (2010)
17. R. R. Adzic, M. W. Hsiao, E. B. Yeager, J. Electroanal Chem Interfacial Electrochem **260**, 475 (1989)
18. Y. Wang, E. Laborda, B. J. Plowman, K. Tschulik, K. R. Ward, R. G. Palgrave, C. Damm, R. G. Compton, Phys. Chem. Chem. Phys. **16**, 3200–3208 (2014)
19. L. A. Larew, D. C. Johnson, J. Electroanal Chem. Interfacial Electrochem **262**, 167 (1989)
20. K. B. Kokoh, J. M. Léger, B. Beden, H. Huser, C. Lamy, Electrochim. Acta **37**, 1909 (1992)
21. M. P. Mercer, D. Plana, D. J. Fermín, D. Morgan, N. Vasiljevic, Langmuir **31**, 10904 (2015)
22. J. Hernández, J. Solla-Gullón, E. Herrero, J. Electroanal. Chem. **574**, 185 (2004)
23. N. Zakharchuk, S. Meyer, B. Lange, F. Scholz, Croat. Chem. Acta **73**, 667 (2000)
24. A. Hamelin, J. Lipkowski, J. Electroanal. Chem. Interfacial Electrochem **171**, 317 (1984)
25. A. Hamelin, J. Electroanal. Chem. Interfacial Electrochem **165**, 167 (1984)
26. K. Engelsmann, W. J. Lorenz, E. Schmidt, J Electroanal Chem Interfacial Electrochem **114**, 1 (1980)
27. K. Engelsmann, W. J. Lorenz, E. Schmidt, J Electroanal Chem Interfacial Electrochem **114**, 11 (1980)
28. W. Zhang, H. Lin, H. Lu, D. Liu, J. Yin, Z. Lin, J. Mater. Chem. A **3**, 4399 (2015)